Influence of High Strain Rates on the Mechanical Behavior of High Manganese Steels

A. Khosravifard

Department of Materials Engineering, Shiraz Branch, Islamic Azad University, Shiraz 71955, Iran

Abstract: In this study, dynamic mechanical properties of three high-manganese steels with TRIP/TWIP or fully TWIP characteristics are studied. High strain rate experiments in the range of true strain rates between ~500 and 1800 /s were conducted using a dynamic torsional testing setup. All the three steels show a positive strain rate sensitivity in the intermediate range of strain rates (up to 500 /s). But, they behave differently as the strain rate is further increased. The steel with the lowest carbon content shows a strain rate softening behavior, while the other two exhibit strain rate hardening. The adiabatic temperature rise of the material greatly influences its stacking fault energy during the high rate dynamic deformation. Thus, unlike the quasi-static experiments, the dominant deformation mechanism of the steel during a dynamic test changes as the deformation progresses. In this regard, the variations of the stacking fault energy during the deformation are calculated for the three steels.

1. Introduction

Advanced high strength steels (AHSS) have been the subject of numerous recent research studies [1,2]. Various subcategories of AHSS, including dual-phase (DP), multi-phase (MP), transformation induced plasticity (TRIP), and twinning induced plasticity (TWIP) steels have recently been considered in automotive industries in order to reduce the cars' weight while maintaining passengers' safety [3]. TWIP steels contain a high concentration (15-30 wt%) of manganese which prevents the formation of ferrite upon cooling of austenite to room temperature. Furthermore, small concentrations (0-3 wt%) of aluminum and silicon may also be added to control the stacking fault energy (SFE) of the steel. The addition of Al increases the SFE of the steel, while Si reduces it [4]. It has been shown that the plastic deformation of FCC alloys with an SFE in the range of 12-35 mJ/m^2, is accompanied by the formation of mechanical twins [5, 6]. The mechanical behavior of TWIP steels is highly dependent on the inherent characteristics of the steel such as its chemical composition and microstructure, and also on the testing conditions such as strain rate and temperature. At room temperature and quasi-static conditions, TWIP steels usually show an ultimate tensile strength in the range of 700-1500 MPa with an elongation of 30-60% [7]. This unique combination of strength and ductility is attributed to the mechanical twinning which leads to high rates of work hardening in TWIP steels [8].

The influence of strain rate on the quasi-static behavior of TWIP steels has been studied by a number of researchers. Lebedkina et al. [9] conducted quasi-static tensile tests on a TWIP steel and found a negative coefficient of strain rate sensitivity in the range of strain rates from about 10^{-5} to 10^{-2} /s. Chung et al. [10] also obtained similar results in tensile and compressive experiments on high manganese TWIP

steel. The negative strain rate sensitivity of TWIP steels at quasi-static conditions has been mainly ascribed to dynamic strain aging (also known as the Portevin-Lechatlier effect) [7].

There exist relatively fewer studies on the mechanical behavior of TWIP steels at high strain rate regime (>100 /s). Split-Hopkinson experiments are the most widely used and reliable techniques for testing the materials in the strain rate range of 10^2 to 10^4 /s [11]. Grassel et al. [12] conducted tensile Hopkinson tests on a Fe-25Mn-3Si-3Al TWIP steel and studied its behavior at strain rates of up to 1000/s. They concluded that as the strain rate increases, the rate of increase of UTS is lower than that of the yield strength (YS) of the steel. By performing split-Hopkinson compressive experiments, Sahu et al. [13] showed that the adiabatic temperature rise during dynamic deformation of a TWIP steel affects the stability of austenite in the steel. It is also suggested that the increase of temperature enhances the dislocation glide mechanism during the plastic deformation of steels with low SFE [7]. Furthermore, the temperature rise leads to an increase of the SFE [14, 15]. Therefore, as the temperature of a TWIP steel increases, the generation rate of mechanical twins is expected to decrease. On the other hand, Li et al. [16] reported an increase in the density of generated twins as the strain rate increased. It can be concluded that the influence of strain rate on the mechanical behavior of low SFE steels still remains challenging.

In the present study, the mechanical behavior of three high manganese (> 20 wt%) steels with either fully TWIP or combined TRIP/TWIP characteristics are surveyed. High strain rate torsional experiments are performed on the steels within the range of true strain rates from ~500 to 2000 /s. The quasi-adiabatic temperature rising during dynamic deformation of the steels is evaluated and its influence on the SFE and mechanical behavior of the steels is investigated.

2. Experimental procedure

Three high-Mn steels with the chemical compositions presented in Table 1 were cast in a laboratory induction furnace. The concentration of carbon in the alloys varied between 0.07 and 0.49 wt%. Based on their carbon contents (high, medium and low), the steels were designated as HC, MC and LC steel, respectively. All the three steels contained over 20 wt% manganese. The cast ingots were homogenized at a temperature between 1100 and 1150 °C. Subsequently, the ingots were hot rolled in three passes from an initial thickness of 43-47 mm to the final thickness of 18 mm.

All of the dynamic experiments were performed using a high strain rate torsional testing machine. The schematic representation of the test setup is shown in Figure 1. The specimen was placed between the incident and transmitter bars. The elastic torsional pulses which travel along the bars were measured using two Wheatstone bridges made of resistance strain gauges (gauge 1 & 2 in Fig. 1). The stress, strain and strain rate which were applied to the specimen were calculated using the recorded elastic pulses. Detailed description of the design and operation of the machine was presented in a previous work [17].
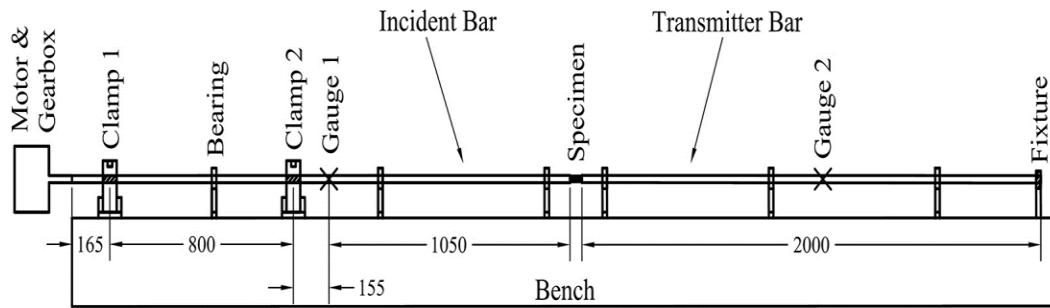
Fig. 1. Schematic representation of the high strain rate torsional testing machine used in the present study (all dimensions in mm).

Torsional specimens were machined out of the hot rolled steels using the WEDM technique according to the plan of Figure 2. The gauge lengths (l_0) of different specimens varied between 1 and 3 mm.
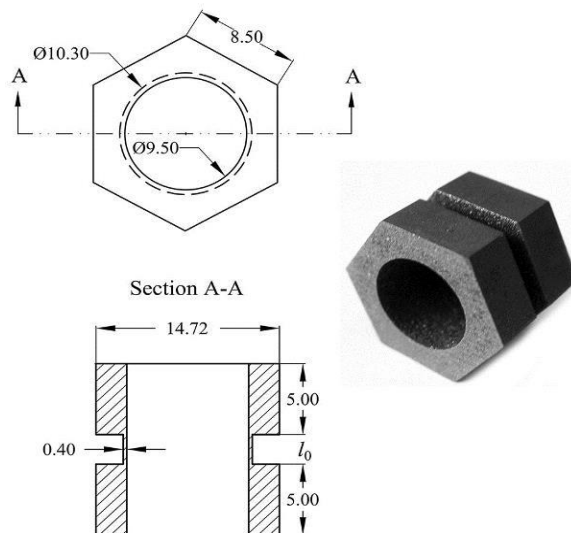

Fig. 2. Torsional specimens used in the high strain rate tests.

3. Results and discussion

3.1. Elastic torsional pulses

The instantaneous values of shear strain rate during a test are inversely proportional to the gauge length of the specimen [18]:

$$\dot{\gamma}_s(t) = \frac{r_s}{l_0}\left[\dot{\theta}_1(t) - \dot{\theta}_2(t)\right] \tag{1}$$

Where $\dot{\theta}_1(t)$ and $\dot{\theta}_2(t)$ are the angular velocities of the specimen ends, and r_s is the mean radius of the thin-wall specimen. Thus, in order to apply different values of strain rate, specimens with various gauge lengths were tested, while the twist angle of the incident bar was kept constant.

During each test, with the sudden release of clamp 2 (Fig. 1), the torque which had been stored in the incident bar was released. Half of the torque traveled towards the specimen and the other half towards clamp 1. Thus, a torsional pulse reached gauge 1 and initiated the so-called incident pulse. As the torsional pulse crashed the specimen, a part of it was reflected back towards gauge 1, while another part was transmitted through the specimen and entered the transmitter bar. The above mentioned pulses are called the reflected and transmitted pulses which are measured by gauges 1 and 2, respectively. On the other hand, the torque which traveled towards clamp 1, is reflected back with a reverse direction and makes endpoints to the incident, reflected and transmitted pulses. Regarding the torsional testing setup used in this study, a time interval of approximately 500 μsec was expected between the initiation and end points of the transmitted pulse, provided that the specimen did not fail during the test [17]. The torsional pulses which were recorded for the 1 and 2-mm long specimens of MC steel, as typical samples, are depicted in Fig. 3. In case of the 1-mm long specimen, the transmitted pulse has initiated at $t \cong 700\,\mu\sec$ and ended at $t \cong 1100\,\mu\sec$.
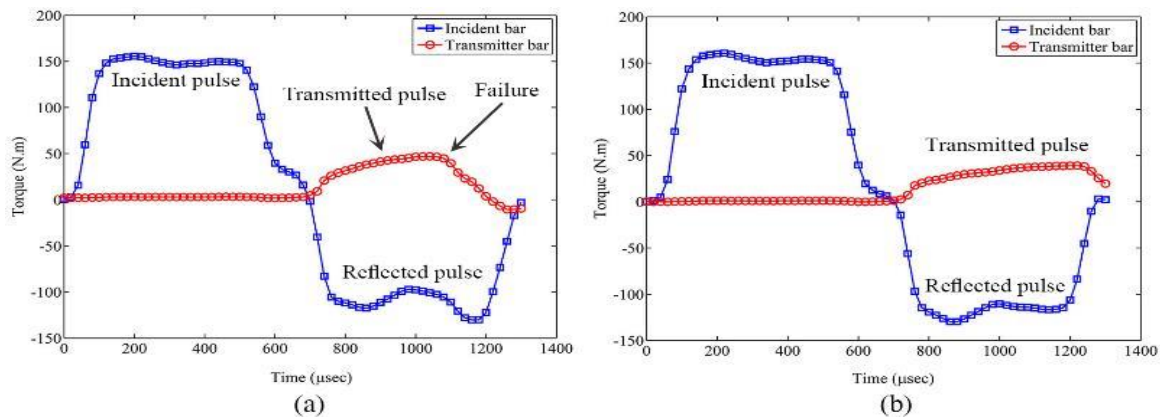

Fig. 3. Torsional pulses recorded on the incident and transmitter bars during testing the typical specimens of MC steel with the gauge length of a) 1 and b) 2 mm.

Thus, it can be deduced that the 1-mm long specimen has failed after about 400 μsec. In contrast, the 2-mm long specimen experienced a smaller strain and did not fail until the end of the transmitted pulse ($t \cong 1200\,\mu\sec$).

3.2. Dynamic mechanical behavior of the steels

The shear stress-strain data obtained for the three steels were converted to true quantities by multiplying the shear stress and division of the shear strain by $\sqrt{3}$. The true stress values at 5, 15, and 25% true strain were plotted versus logarithmic strain rate as shown in Fig. 4.
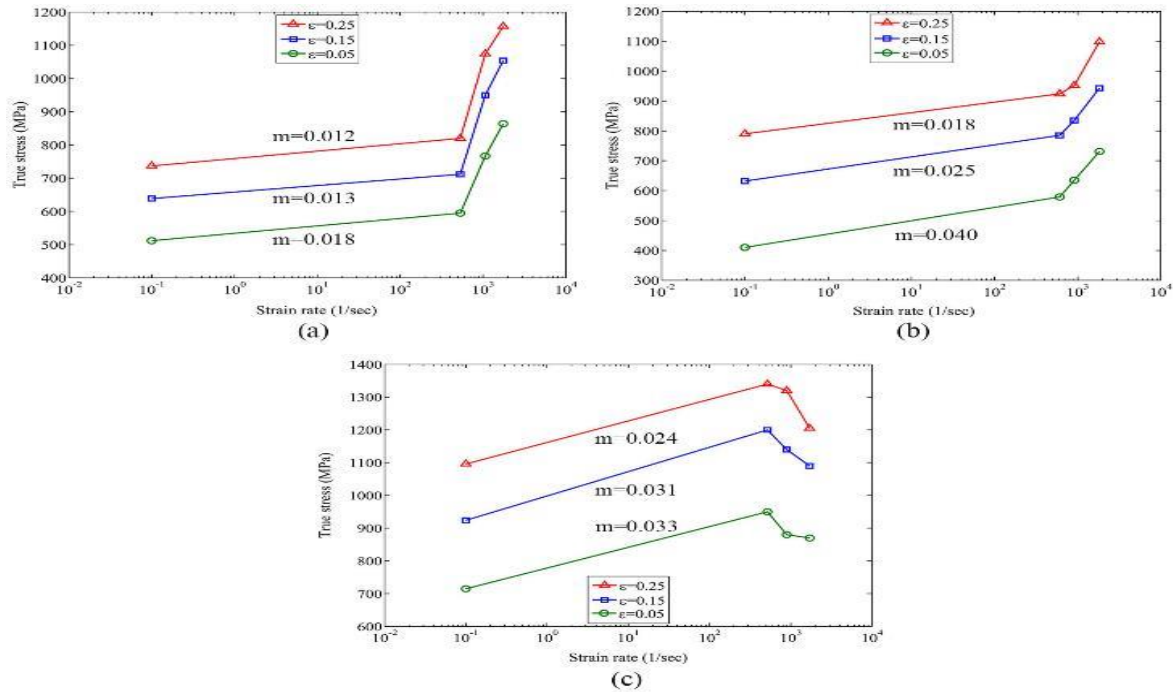
Fig. 4. True stress values at 5, 15 and 25% true strain versus logarithmic strain rate for
a) HC, b) MC, and c) LC steel.

Within the intermediate range of strain rates $(0.1 \leq \dot{\varepsilon} \leq 600 / \text{sec})$, typical strain rate hardening behavior was observed for all the three steels. The measured values of relative strain rate sensitivity $(m = d \ln \sigma / d \ln \dot{\varepsilon})$ are also shown for the three steels in Figure 4. The values of m for the investigated steels varied between 0.012 and 0.04 within the above range of strain rates.

As the strain rate was further increased, the steels behaved quite differently. In the high strain rate range $(600 < \dot{\varepsilon} < 1700 / \text{sec})$, the HC and MC steels exhibited a positive strain rate sensitivity. A steep upturn in the flow stress was observed for both steels. This is usually attributed to the viscous drag effects which influence the movement of dislocations at high strain rates [19]. Due to relatively lower carbon and manganese contents of the LC steel, its room temperature microstructure consisted of a duplex mixture of austenite and epsilon martensite [20]. As the result of presence of martensite, the flow stress levels were higher for the LC steel compared to the MC and HC steels (Fig. 4). However, in case of the LC steel, a slight strain rate softening behavior was seen in this range of strain rates. Regarding the very low SFE of the LC steel, its plastic deformation was initially accompanied by transformation of the retained austenite to martensite (TRIP effect). On the other hand, increasing the strain rate decreased the effective pulse duration. In other words, as the strain rate increased, there was a shorter period of time for microstructural evolutions (such as the martensitic transformation) to occur up to a certain value of strain [21]. As the result, a strain rate softening behavior was observed for the LC steel. This has been further discussed in an earlier work [22]. Another possible reason for the different effects of high strain rates on the mechanical behavior of the studied steels originates from the different impacts of the solute drag effects in these steels. It has been stated that the drag effects increase as the concentrations of the alloying elements (mainly carbon and manganese) increase [23]. In consistence, the strain rate hardening behavior observed

for the HC steel has been the highest. Furthermore, as proposed by Saeed-Akbari et al. [24], increasing the carbon content of a high-Mn steel increases the possibility of formation of CMn_6 clusters. These ordered clusters also contribute to the drag effects on the moving dislocations. It should be also noted that the higher strain rate is achieved with the shorter specimen. It has been shown elsewhere [17] that inhomogeneity of the deformation in the 1-mm specimen of the LC steel introduces a considerable softening effect in this specimen.

The mechanical behavior of high-Mn steels is commonly explained regarding the work hardening rate ($d\sigma/d\varepsilon$) and its variation with the progress of the deformation. The curves of work hardening rate versus true strain were obtained for the three steels by calculating numerical differentiation of the true stress with respect to true strain. The resultant curves were first smoothed and then plotted for different strain rates (~500 to 1800 /sec) as shown in Figure 5.
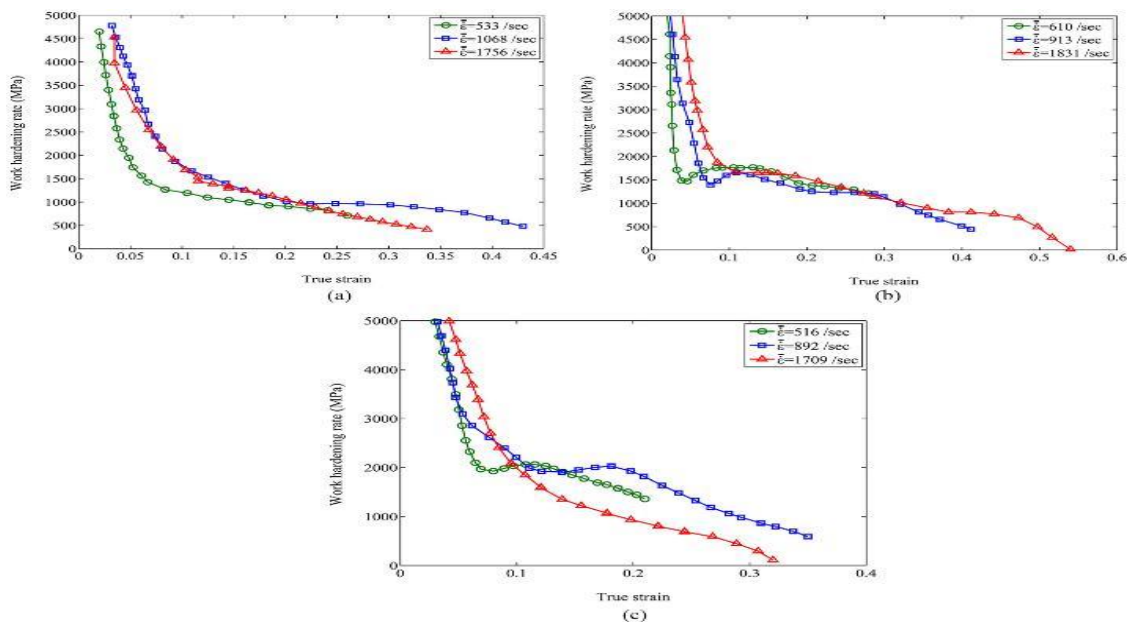

Fig. 5. Work hardening rate curves obtained at different strain rates for a) HC steel, b) MC steel, and c) LC steel.

After the initial high work hardening which was seen for all the three steels, they exhibited different hardening rates with the increase of strain. The work hardening rate of the HC steel rapidly fell to about 1000 MPa, but it remained almost constant up to the true strain of ~0.3. At the high strain rate of 1756 /sec, a continuous decrease of the work hardening rate was observed. In case of the MC steel, after the initial hardening, work hardening rates at different strain rates reduced to values between 1500 and 1700 MPa. Afterwards, a slight increase was seen for the hardening rate. At all the three strain rates, the hardening rate was quite high up to the true strains of approximately 0.3. The approach of the hardening curves which were obtained for the LC steel at the strain rates of 516 and 892 /sec, were similar to those obtained for the MC steel. However, the values were slightly higher (~ 2000 MPa) up to the true strain of ~0.2. In case the high strain rate of 1709 /sec, a continuous decrease of the hardening rate was observed for the LC steel.

Within the quasi-static range of strain rates, values between ~1500 to 2500 MPa have been reported in the literature for the work hardening rates of TRIP/TWIP and TWIP steels [25, 26, 27]. These values are reasonably close to the results obtained at dynamic conditions in the present work. However, by comparison, it can be seen that the high rates of work hardening at quasi-static conditions has been maintained up to slightly larger values of true strain (~0.4) [26]. This is related to the adiabatic temperature rise during dynamic deformation of materials and will be further discussed below.

As the dominant mechanism of plastic deformation is highly dependent on the stacking fault energy (SFE), the SFE of the three steels were calculated through a thermodynamic approach [17]. The SFE values obtained at room temperature for the HC, MC, and LC steels were 28, 14, and 4 mJ/m^2, respectively. However, during a high rate deformation, the temperature of the material adiabatically increases. The amount of the temperature rise can be calculated by a simple balance of energy through the following equation [21]:

$$\Delta T = \beta \int \sigma . d\varepsilon \, /(\rho C_p)$$ (2)

In this equation, β, is the Taylor-Quinney parameter, ρ, is the density and C_p, is the specific heat capacity of the tested material. The values of adiabatic temperature rise were calculated for the three steels according to equation (2). These are demonstrated in Figures. 6a-c. The Taylor-Quinney parameter was taken as 1.0 at all the high strain rates. Expectedly, the temperature of the tested materials increased with the progress of strain. The amount of the temperature rise obtained up to a certain value of strain was the highest for the LC steel. This is due to higher flow stresses of this steel which can be attributed to the presence of martensite in its microstructure.

The temperature rise leads to thermal softening and increase of the SFE. The increased SFE could be calculated through the temperature dependent thermodynamic quantities as presented and discussed by Saeed-Akbari et al. [28] and Dumay et al. [6]. The variation of SFE versus temperature is shown in Fig. 6d for the studied steels.

The value of SFE for the HC steel was initially below the critical value of 35 mJ/m^2, i.e. mechanical twinning was expected to be the main mechanism during its plastic deformation. However, after experiencing a small amount of strain, the SFE of this steel exceeded the range of domination of mechanical twinning. As a result, the hardening rates were the lowest for this steel (Figure 5). On the other hand, the SFE of the MC steel did not exceed the critical value up to large values of strain (~0.5). Consistently, the hardening rate of this steel was considerably higher than that of the HC steel. In case of the LC steel, the SFE was initially very low (4 mJ/m^2). Since the plastic deformation of the steel at room temperature would be mainly accompanied by the martensitic transformation, the hardening rates of this steel were initially higher than the other steels (Fig. 5).
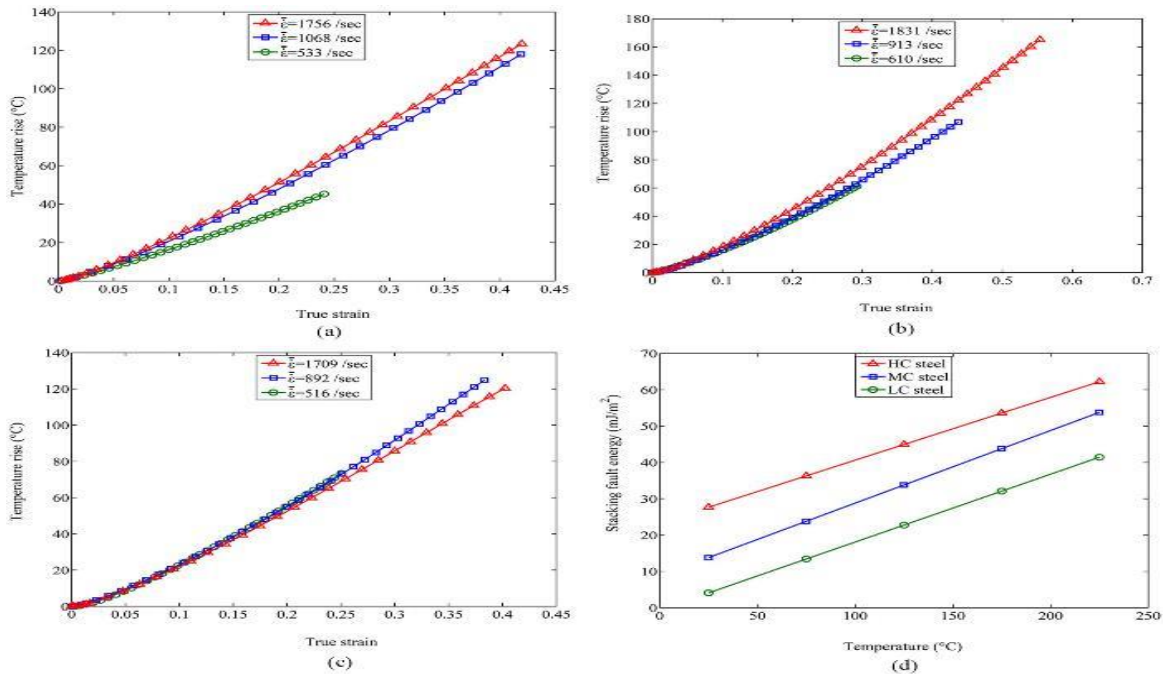
Fig. 6. The adiabatic temperature rise during dynamic deformation of a) HC steel, b) MC steel, c) LC steel, and d) the variation of SFE with temperature for the three steels.

Furthermore, the initial microstructure of the LC steel consisted of some martensite which could contribute to higher initial work hardening of this steel. With the progress of the dynamic deformation, its temperature increased and so did the SFE. Thus, after a certain value of strain, mechanical twinning became the dominant deformation mechanism. A considerable fraction of the austenite phase which was initially present in the microstructure of the steel transformed into martensite. Therefore, a relatively lower amount of austenite was available in this steel for the occurrence of mechanical twinning. As a result, the hardening rate of this steel started to decrease after a true strain of ~0.2. The rate of work hardening at the highest strain rate of 1709 /sec, exhibited a continuous decrease which is due to both the adiabatic temperature rise and shorter deformation pulse duration.

4. Conclusion

The dynamic mechanical behavior of three high manganese steels was studied using a high strain rate torsional testing machine. High strain rates in the range of ~500 to 1800 /s were applied to the three steels and the following main conclusions could be drawn:

1. Shorter transmitted pulse was acquired in the case of the specimen with shorter gauge length which failed as the result of higher strain rate and strain.
2. All the three steels have shown a positive strain rate sensitivity of about 0.012 to 0.04 within the intermediate strain rate range (up to ~500 /s). However, as the strain rate was increased to ~1800 /s, the LC steel showed a slight strain rate softening behavior.
3. The HC steel showed the minimum work hardening rates due to its highest stacking fault energy (SFE).

4. The work hardening rate of the LC steel was initially higher due to its martensite content. However it started to decrease after a true strain of about 0.2 which was ascribed to its increased SFE due to adiabatic temperature rise.

5. The MC steel showed quite high hardening rate up to the true strains of ~0.3, since its SFE did not exceed the upper limit for the occurrence of mechanical twinning.

5. References

[1] A. S. Khan, M. Baig, S. H. Choi, H. S. Yang and X. Sun, Quasi-static and dynamic responses of advanced high strength steels: Experiments and modeling, *International Journal of Plasticity*, 30-31 (2012) 1-17.

[2] R. Kuziak, R. Kawalla and S. Waengler, Advanced high strength steels for automotive industry, *Archives of Civil and Mechanical Engineering*, 8 (2008) 103-117.

[3] V. J. Slycken, P. Verleysen, J. Degrieck, J. Bouquerel and B. C. De Cooman, Dynamic response of aluminum containing TRIP steel and its constituent phases, *Material Science and Engineering A*, 460–461 (2007) 516–524.

[4] R. E. Schramm and R. P. Reed, Stacking fault energies of seven commercial austenitic stainless steels, *Metallurgical Transactions A*, 6 (1975) 1345-1351.

[5] S. Allain, J. P. Chateau, O. Bouaziz, S. Migot and N. Guelton, Correlations between the calculated stacking fault energy and the plasticity mechanisms in Fe–Mn–C alloys, *Materials Science and Engineering A*, 387–389 (2004) 158-162.

[6] A. Dumay, J. P. Chateau, S. Allain, S. Migot and O. Bouaziz, Influence of addition elements on the stacking-fault energy and mechanical properties of an austenitic Fe–Mn–C steel, *Materials Science and Engineering A*, 483–484 (2008) 184-187.

[7] O. Bouaziz, S. Allain, C. P. Scott, P. Cugy and D. Barbier, High manganese austenitic twinning induced plasticity steels: A review of the microstructure properties relationships, *Current Opinion in Solid State and Materials Science*, 15 (2011) 141–168.

[8] L. Remy, Kinetics of f.c.c. deformation twinning and its relationship to stress-strain behaviour, *Acta Metallurgica*, 26 (1978) 443-451.

[9] T. A. Lebedkina, M. A. Lebyodkin, J. P. Chateau, A. Jacques and S. Allain, On the mechanism of unstable plastic flow in an austenitic FeMnC TWIP steel, *Materials Science and Engineering A*, 519 (2009) 147–154.

[10] K. Chung, K. Ahn, D. H. Yoo, K. H. Chung, M. H. Seo and S. H. Park, Formability of TWIP (twinning induced plasticity) automotive sheets, *International Journal of Plasticity*, 27 (2011) 52–81.

[11] T. George, Classic Split-Hopkinson Pressure Bar Testing, in ASM Handbook, Vol. 8, *Mechanical Testing and Evaluation*, ASM International, Materials Park, Ohio, 2000, pp.1027-1068.

[12] O. Grassel, L. Kruger, G. Frommeyer and L. W. Meyer, High strength Fe-Mn-(Al, Si) TRIP/TWIP steels development-properties-application, *International Journal of Plasticity*, 16 (2000) 1391-1409.

[13] P. Sahu, S. Curtze, A. Das, B. Mahato, V. T. Kuokkala and S. G. Chowdhury, Stability of austenite and quasi-adiabatic heating during high strain-rate deformation of twinning-induced plasticity steels, *Scripta Materialia*,

62 (2010) 5–8.

[14] A. Soulami, K. S. Choi, Y. F. Shen, W. N. Liu, X. Sun and M. A. Khaleel, On deformation twinning in a 17.5% Mn–TWIP steel: A physically based phenomenological model, *Materials Science and Engineering A*, 528 (2011) 1402–1408.

[15] A. Imandoust, A. Zarei-Hanzaki, M. Sabet and H. R. Abedi, An analysis of the deformation characteristics of a dual phase twinning-induced plasticity steel in warm working temperature regime, *Materials and Design*, 40 (2012) 556–561.

[16] D. Li, Y. Wei, C. Lid, L. Hod, D. Lid and X. In, Effects of High Strain Rate on Properties and Microstructure Evolution of TWIP Steel Subjected to Impact Loading, *Journal of Iron and Steel Research, International*, 17 (2010) 67-73.

[17] A. Khosravifard, M. M. Moshksar and R. Ebrahimi, High strain rate torsional testing of a high manganese steel: *Design and simulation, Materials and Design*, 52 (2013) 495-503.

[18] A. Gilat, Torsional Kolsky Bar Testing, in ASM Handbook, Vol. 8, Mechanical Testing and Evaluation, *ASM International, Materials Park, Ohio*, 2000, pp.1134-1162.

[19] S. Curtze and V. -T. Kuokkala, Dependence of tensile deformation behavior of TWIP steels on stacking fault energy, temperature and strain rate, *Acta Materialia*, 58 (2010) 5129-5141.

[20] A. Khosravifard, A. S. Hamada, M. M. Moshksar, R. Ebrahimi, D. A. Porter, L. P. Karjalainen, High temperature deformation behavior of two as-cast high-manganese TWIP steels, *Materials Science & Engineering A*, 582 (2013) 15-21.

[21] Z. P. Xiong, X. P. Ren, W. P. Bao, S. X. Li and H. T. Qu, Dynamic mechanical properties of the Fe−30Mn−3Si−4Al TWIP steel after different heat treatments, *Materials Science and Engineering A*, 530 (2011) 426–431.

[22] A. Khosravifard, M. M. Moshksar and R. Ebrahimi, Mechanical Behavior of TWIP Steel in High Strain Rate Torsional Test, *International Journal of ISSI*, 9 (2012) 15-19.

[23] M. Itabashi and K. Kawata, Carbon content effect on high-strain-rate tensile properties for carbon steels, *International Journal of Impact Engineering*, 24 (2000) 117-131.

[24] A. Saeed-Akbari, L. Mosecker, A. Schwedt and W. Bleck, Characterization and Prediction of Flow Behavior in High-Manganese Twinning Induced Plasticity Steels: Part I. Mechanism Maps and Work-Hardening Behavior, *Metallurgical and Materials Transactions A*, 43 (2012) 1688-1704.

[25] D. Barbier, N. Gey, S. Allain, N. Bozzolo and M. Humbert, Analysis of the tensile behavior of a TWIP steel based on the texture and microstructure evolutions, *Materials Science and Engineering A*, 500 (2009) 196–206.

[26] H. Ding, H. Ding, D. Song, Z. Tang and P. Yang, Strain hardening behavior of a TRIP/TWIP steel with 18.8% Mn, *Materials Science and Engineering A*, 528 (2011) 868–873.

[27] I. Gutierrez-Urrutia and D. Raabe, Dislocation and twin substructure evolution during strain hardening of an Fe–22 wt.% Mn–0.6 wt.% C TWIP steel observed by electron channeling contrast imaging, *Acta Materialia*, 59 (2011) 6449–6462.